Sequences Responsible for Intracellular Localization of β-Actin Messenger RNA Also Affect Cell Phenotype

Edward H. Kislauskis, Xiaochun Zhu, and Robert H. Singer

Department of Cell Biology, University of Massachusetts Medical Center, Worcester, Massachusetts 01655

Abstract. We have characterized the structure and function of RNA sequences that direct β-cytoplasmic actin mRNA to the cell periphery were mapped to two segments of 3'-untranslated region by expression of LacZ/β-actin chimeric mRNAs in chicken embryo fibroblasts (CEFs). A 54-nt segment, the "RNA zipcode," and a homologous but less active 43-nt segment each localized β-galactosidase activity to the leading lamellae. This zipcode contains the full activity, and mutations or deletions within it reduce, but do not eliminate, its activity, indicating that several motifs contribute to the activity. Two of these motifs, when multimerized, can regenerate almost full activity. These sequences are highly conserved in evolution, since the human β-actin zipcode, positioned identically in the 3'UTR localizes equally well in chicken cells. Complementary phosphorothioate oligonucleotides against the zipcode delocalized endogenous β-actin mRNA, whereas those complementary to the region just outside the zipcode, or sense oligonucleotides, did not. Actin mRNA or protein levels were unaffected by the antisense treatments, but a dramatic change in lamellipodia structure, and actin stress fiber organization was observed using the same antizipcode oligonucleotides which delocalized the mRNA. Hence, discrete 3'UTR sequences direct β-actin isoform synthesis to the leading lamellae and affect cell morphology, presumably through the actin cytoskeleton.

ACTIN is a highly abundant structural constituent of all eukaryotic cells integral to a variety of cellular functions. As a major constituent of the cytoskeleton or myofilaments, it is essential for the maintenance of cell polarity and motility (Bretcher, 1991; Cooper, 1991; Levitt et al., 1987; Pollard and Goldman, 1993), intracellular transport (Kuznetsov et al., 1992), protein synthesis (Hesketh and Pryme, 1991; Negrutskii and Deutscher, 1991; Yang et al., 1990), enzymatic processes (Farwell et al., 1990; Hunt et al., 1990; Knull and Walsh, 1992; Sarndahl et al., 1989), and mRNA localization (Singer, 1992; Sundell and Singer, 1991; Yisraeli et al., 1990). In chicken embryonic fibroblasts and myoblasts, actin mRNA is highly localized at the leading lamellae, quite different from the distribution of mRNAs coding for either vimentin or tubulin (Lawrence and Singer, 1986). In leading lamellae, rapid changes in actin polymerization drive extension of the lamellipodia (Carlier, 1991; Cooper, 1991; Wang, 1987). Both β-actin protein and mRNA colocalize at the leading edge of endothelial cells in response to wounding (Hoock et al., 1991) and in C2 myoblasts (Hill and Gunning, 1993). Thus, actin mRNA localization may facilitate the compartmentalization of actin synthesis (Singer, 1992). The ability of β-actin mRNA to be transported and to anchor at the leading lamellae does not require new protein synthesis and, hence, must involve *cis*-acting elements on the mRNA (Sundell and Singer, 1990). Recent work indicated that the β-actin RNA localization signal ("zipcode") is contained within the 3'UTR and not in either the 5'UTR or the coding region (Kislauskis et al., 1993; Singer, 1993).

The precise characterization of essential RNA localization determinants is a prerequisite for understanding the mechanism by which mRNAs are localized, and elucidating the functional significance of this localization. Therefore, we understood an extensive analysis of the *cis*-acting sequences responsible for this process. These sequences were isolated using a transfection assay wherein coding sequences for β-galactosidase were fused to sequences derived from the chicken β-cytoplasmic actin cDNA. The percent of cells which showed peripheral localization of the enzymatic activity was quantitatively monitored and provided a rigorous evaluation of each construct. Statistically, significant differences in the localization capacity of various segments of the β-actin cDNA could be distinguished by this approach. Importantly, anti-sense oligonucleotides complementary to the β-actin RNA zipcode confirmed the physiological importance of this sequence and suggested a role of β-actin mRNA localization in cell morphology.

Address all correspondence to Dr. Edward H. Kislauskis, Department of Cell Biology, University of Massachusetts Medical Center, 55 Lake Avenue North, Worcester, MA 01655. Telephone: (508) 856-4230; FAX: (508) 856-5612.

Materials and Methods

Plasmid Constructions

The plasmid RSVβgal was previously described (Kislauskis et al., 1993). In Fig. 2, construct *A* was constructed by modifying the complete 1814-bp Pst I fragment representing the full-length cDNA clone for chicken cytoplasmic β-actin (Cleveland et al., 1980) with Bam HI linkers (GIBCO BRL, Gaithersburg, MD) and inserting it into the RSVβgal polylinker. Construct B was also inserted as a Bam HI fragment after the exo III/mungbean nuclease (Promega, Madison, WI) deletion of 3' sequences to position 1452, leaving 233 nucleotides (nt)[1] of 3'UTR. Construct C was created by inserting β-actin sequences from 1-1278 as a Bam HI–Xba I fragment after the addition of Xba I linkers at the Fsp I site (1278). Construct D β-actin sequences from 1193-1814, was inserted as a Bam HI fragment as a biproduct of construction of construct E. Construct E containing β-actin sequences from 1-1192 was inserted as a Bam HI fragment by modifying the Ava II site at position 1192 with Bam HI linkers. Construct F was inserted as a 483-nt Mbo I fragment into the Bam HI site of RSVβgal. Construct J was created by joining a Bam HI–Xba I fragment (1-1192) of construct E with Xba I–Not I fragment generated by PCR using the upper primer 5'-GGACTAGATGCGCATAAAACAAGACG and the lower primer 5'-TTGCGGCCGCTCAGTGTACAGGTAGCCCCT and corresponding to positions to β-actin positions 1275-1778. Construct K was constructed from a PCR-generated fragment using the upper primer 5'-GGACTAGATGCGCATAAAACAAGACG and the lower primer 5'-TTGCGGCCGCTCAGTGTACAGGTAGCCCCT which converted the Fsp I site at position 1278 to an Xba I site and generated a 507-bp Xba I–Not I fragment. Construct M the double mutant, was synthesized by connecting construct E with two PCR-generated fragments: one corresponding to positions 1278-1419 as a 153-bp Xba I–Hind III fragment using the upper primer 5'-GGTCTAGAGCATAAAACAAGACGAGATTG and the lower primer 5'-GGAAGCTTAGAACTTTGGGGGCGT; and the other corresponding to positions 1453-1778 as a 337-bp Hind III–Not I fragment using the upper primer 5'-TTGGGCGCTATTGTGTGCACTTTTATTT and the same lower primer used to create construct K. Constructs G–I, L, and N–Q were synthesized as complementary pairs of oligonucleotides flanked by linker sequences (Bam HI and Xba I at the 5' and 3' ends, respectively) allowed for directional cloning into the vector once annealed. The following pair of oligos were annealed and inserted between the Bam HI and Xba I sites in RSVβgal to create construct G: 5'-GATCCTAAACCGGACTGTTACCAACACCCACACCCTGTGATGAAACACCCCCCATAAATGCT and 5'-CTAGAGCATTTATGGGTTTTGTTTCATCACAGGGGTGTGGGTGTTGGTAACAGTCCGGTTTAG. Construct H was inserted into the Bam HI site after the annealing of oligo pair: 5'-CATCC*GCAAGCAGGAGTACGATGAATCCGGACCCTCCATTGTCCACCGCAAA and 5'-GATCTTTGCGGTGGACAATGGAGGGTCCGGATTCATCGTACTCCTGCTTGCG* (* = should have been an A residue, not G in sense strand). Construct I was inserted between the Xba I and Not I sites after the annealing of an oligo pair: 5'-CTAGAAACAAGACGAGATTGGCATGGCTTTATTTGTTTTTTCTTTTGC and 5'-GGCCGCAAAAGAAAAAACAAATAAAGCCATGCCAATCTCGTCTTGTTT. The pair of oligos used to create construct Q which was inserted between the BamHI and XbaI site of RSV β gal were: 5'-GATCCTAGGCGGACTATGACTTAGTTGCGTTACACCCTTTCTTGACAAAACCTAACTTGCGCT and CTAGAGCGCAAGTTAGGTTTTGTCAAGAAAGGGTGTAACGCAACTAAGTCATAGTCCGCCTAG. Construct L was similarly prepared using the following oligo pair: 5'-GATCCCAAGTTCTACAATGCATCTGAGGACTTTGATTGTACATTTGTT and CTAGAACAAATGTACAATCAAAGTCCTCAGATGCATTGTAGAACTTGG. These constructs were verified by restriction and sequence analysis using standard methods. Oligo motifs were synthesized, annealed, and ligated into the polylinker as above. The GGACT motif was comprised within the two complementary strands: 5'-GATCCTAAACCGGACTGTA and 5'-AGTCTACAGTCCGGTTTAG; and the AATGC motif was comprised within the two complementary strands: 5'-GATCCAACCCATAAATGCA and 5'-GATCTGCATTTATGGGTTG.

Transfection, In Situ Hybridization, and Immunohistochemistry

Twelve day-old chicken embryonic fibroblasts (CEFs) were prepared using standard techniques and cultured onto gelatin-coated coverslips as previously described (Lawrence et al., 1989; Sundell and Singer, 1990). The transfection, staining, and statistical analysis were done as previously described (Kislauskis et al., 1993). After transfection, cells on coverslips were washed with PBS solution, fixed for 10 min at room temperature in 4% paraformaldehyde in PBS/5 mM $MgCl_2$, rinsed in PBS, and stored in 70% ethanol at 4°C. For methods where enzyme activity and the reporter mRNA were detected simultaneously, nick-translated probes were generated using standard procedures (Lawrence and Singer, 1989). To detect endogenous actin mRNAs, coverslips were hydrated in PBS/5 mM $MgCl_2$, and then hybridized overnight (~12 h) at 37°C with 20 ng of nick-translated digoxigenin-labeled β-actin cDNA sequences 95-1477 (Sundell and Singer, 1990). To detect Lac Z reporter mRNAs, each coverslip was hybridized to 20 ng of digoxigenin-labeled, nick-translated RSVβgal plasmid overnight at 37°C. Anti-digoxigenin conjugated to alkaline phosphatase was diluted 1:250 in PBS containing 2 mg/ml BSA (Boehringer Mannheim Corp., Indianapolis, IN). Alternatively, in a double-label in situ hybridization procedure, a primary antibody anti-digoxigenin HRP to detect endogenous actin mRNA (Boehringer Mannheim) at a 1:250 dilution in PBS plus 0.2% BSA was incubated for 30 min at 37°C, washed, subsequently stained with diaminobenzidine (DAB), and amplified by silver enhancement using the AMP B Silver Enhancement Kit (DIGENE Diagnostics Inc., Silver Spring, MD). This was used simultaneously with the β-galactosidase reaction to identify the distribution of fusion transcript. Cellular actin was stained after fixation with FITC-conjugated phalloidin (Molecular Probes, Inc., Eugene, OR).

Phosphorothioate Antisense Oligonucleotides

Antisense treatment was performed on CEFs grown, as described above, to ~50% confluence in OPTI-MEM I medium (GIBCO BRL) containing 10% FBS. Oligonucleotides were synthesized on a DNA synthesizer model 396 (Applied BioSystems, Foster City, CA), purified through CEPACK columns (Millipore, Milford, MA), lyophilized overnight, and resuspended in DEPC-treated distilled water. Each oligonucleotide was added to the complete medium (Opti-MEM 1 supplemented with 10% FBS). Experiments which required 12-h exposure to these antisense oligonucleotides involved three treatments, 4 h each, in 1.0 ml complete medium. In Fig. 4, oligo A was 5'-TGGTAACAGTCCGGTTTA which corresponded to antisense sequences from the stop codon through the first 15 nt of the 3'UTR (position 1222-1239), oligo B: 5'-TCATCACAGGGGTGTGGGTGT (position 1240-1260), oligo C: 5'GCATTTATGGGTTTTGTT (positions 1261-1278), oligo D: 5'-ATCCTGAGTCAAGCGCCA (positions 1279-1297), oligo E: 5'-CTCAGATCGCTTGTAGAACTT (positions 1412-1432), and oligo F: 5'-AACAAATGTACAATCAAAGTC (positions 1433-1453). Oligo C+ complements oligo C and corresponded to the sense (mRNA) sequence (positions 1261-1278).

RNA and Protein Electrophoresis

Total RNA was extracted from CEFs as previously described (TRI Reagent, Cincinnati, OH), and resolved in a 1% agarose/2.2 M formaldehyde gel before blotting onto ZetaProbe (BioRad Labs., Hercules, CA). One blot was hybridized overnight to ^{32}P-labeled antisense riboprobe generated from the human GAPDH cDNA insert (Clonetech, Palo Alto, CA) at 37°C, washed, and exposed 30 min to film without a screen. Subsequently, chemiluminescence was performed to detect actin mRNA on the same blot. Initially the blot was stripped in 5 mM EDTA for 50 min in boiling water, and then prehybridized at 37°C in 50% formamide, 5× SSC, 0.5% SDS, 5× Denhardt's, and 50 mM $NaPO_4$ for 2 h. Digoxigenin-labeled actin probes (250 ng) were added and hybridized at 37°C for 12 h in the prehybridization solution plus 1% dextran sulfate. The filter was washed as described above, and then in 1% Blocking Reagent in 150 mM NaCl/50 mM Tris pH 7.5 (buffer 1, Boehringer Mannheim) for 30 min at room temperature (RT). Anti-digoxigenin conjugated to alkaline phosphatase (Boehringer Mannheim) was diluted (1:2,500) in 20 ml of blocking buffer and incubated for 30 min at RT. The unbound antibody was washed from the filter, and the filter was rinsed in buffer 3 without $MgCl_2$, and chemiluminescent substrate was diluted (Immunolite Assay Kit, Biorad Labs.), and the blot was incubated in the presence of the substrate for 5 min at RT before exposing it to film at RT. A separate preparation of total RNA from similarly treated CEFs was blotted as above and probed with gel-isolated, random-primed, β-actin 3'UTR sequence (positions 1193-1814) with specific activity of 5×10^6 cpm/ml (Boehringer Mannheim), washed as described above, and exposed to film for 1 h at −80°C.

CEFs were labeled after a 12-h treatment with the various oligonucleotides for 30 min with 150 μCi/ml L-[^{35}S]methionine (Amersham Corp., Arlington Heights, IL) in MEM supplemented with L-leucine and L-lysine

1. *Abbreviations used in this paper*: CEF, chicken embryo fibroblast; NRE, *nos*-responsive element; nt, nucleotide; RT, room temperature.

(GIBCO BRL). Equal TCA-precipitable counts were electrophoresed through 10% SDS-polyacrylamide gel using standard procedures (SEQUAGEL, National Diagnostics, Atlanta, GA). The gel was fixed and silver stained using Silver Stain plus Kit (BioRad Labs.), and then dried, treated with Amplify (Amersham Corp.) for 30 min, and exposed to film at −70°C with enhancing screens. Immunoprecipitation of β-actin involved incubation with saturating concentration of precleared H2 anti-β-actin antisera (10 μl) (Otey et al., 1987) at 4°C overnight on orbital rocker before the addition of 75 μl protein G–Sepharose (Sigma Chem. Co., St. Louis, MO) and an additional 2-h incubation at 4°C. After a brief spin at 14,000 rpm, the pellet was resuspended in 2× sample buffer, boiled for 2 min, and loaded as above.

Results

Structural Properties of the β-Actin RNA Zipcode

Cis-acting RNA determinants responsible for targeting β-actin mRNA to the cell periphery were shown to be capable of conferring peripheral localization to a reporter mRNA encoding β-galactosidase in a transient assay (Kislauskis et al., 1993). To map those sequences to their minimum length, various portions of the chicken β-cytoplasmic actin cDNA were inserted into the polylinker between the *E. coli* LacZ gene and the SV40 3′UTR, in the vector RSVβgal (Fig. 1 *A*). After a transient expression period, CEFs were fixed and stained by a brief (5–15 min) incubation with a chromogenic β-galactosidase substrate, X-gal. The transfection protocol did not affect the localized distribution of endogenous actin mRNA (Fig. 1 *B*). Our "zipcode trap" assay for the presence of zipcode sequences in each construct relied on a significant increase in the number of transfectants with reaction product (*blue stain*) localized to the cell periphery (Fig. 1 *D*) vs those with blue stain distributed throughout the cytoplasm (Fig. 1 *C*).

In nearly all cells (94%) transfected with the vector alone (Fig. 1 *C*), β-galactosidase activity (*blue staining*) was found to be nonlocalized, throughout the cytoplasm. In marked contrast, a significant number of transfectants (33%), expressing reporter transcripts fused to the entire chicken actin cDNA (~1.8 kb), showed blue staining prominently in the peripheral cytoplasm (Fig. 1 *D*). This magnitude was similar to the endogenous level of actin mRNA localization (Kislauskis et al., 1993; Latham et al., 1994). In situ hybridization was performed using probes specific for β-galactosidase coding sequences after staining with X-gal to reveal that the distribution of reporter RNA correlated with the distribution of β-galactosidase activity in the same transfectant. Thus, in-

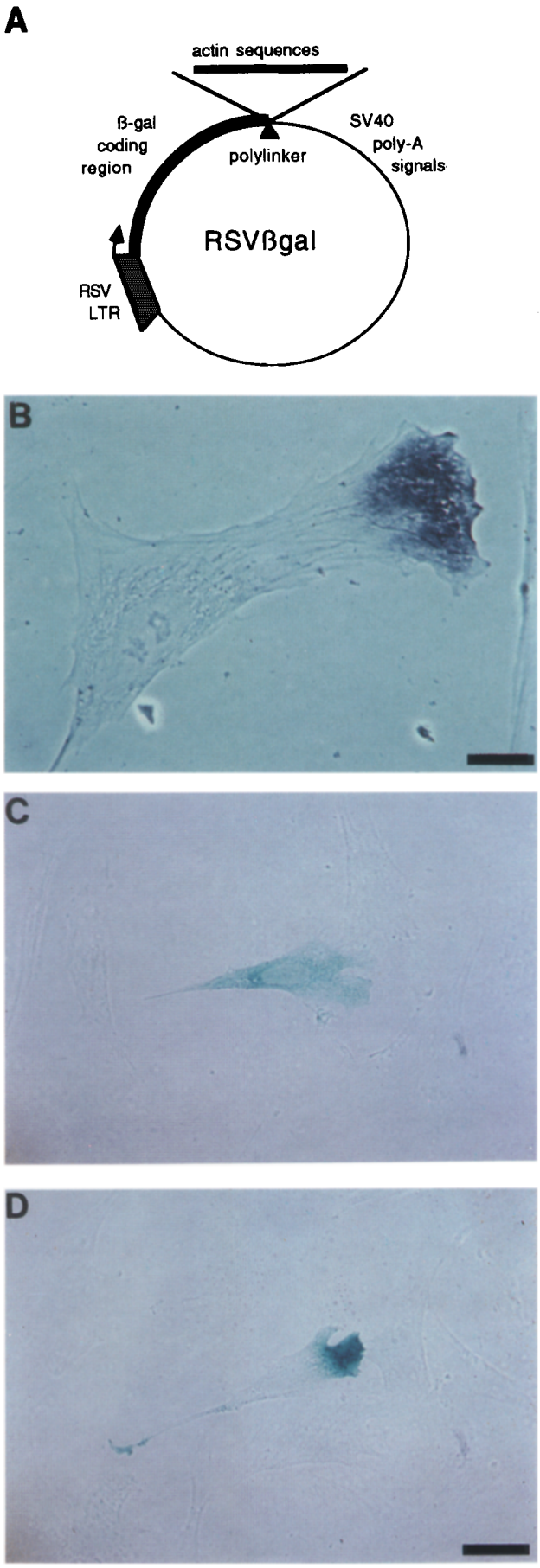

Figure 1. Zipcode Trap expression vector and representative CEF transfectants. (*A*) Schematic of RSVβgal plasmid vector and the site of insertion of actin sequences. Actin sequences are inserted downstream of the β-galactosidase termination codon, thereby extending the 3′UTR of the reporter mRNA. (*B*) Endogenous actin mRNA (*purple*) in a CEF exposed to transfection conditions. Detection was by a digoxigenin-labeled cDNA probe for β-actin mRNA sequences. Actin localization to the leading lamellae, in 40–60% of CEFs, was unaffected by the transfection protocol. Transfected cells are represented in *C* and *D*. The distribution of β-galactosidase activity (*blue staining*) and/or reporter mRNA evident in transfectants after the transient expression of vector (*C*) or the reporter gene fused to the full-length β-actin mRNA (*D*). Bars: (*B*) 10 μm; (*C* and *D*) 20 μm.

tracellular β-galactosidase activity was an accurate indicator of the LacZ mRNA distribution in our transient assay. These data provided a statistically significant basis for assessing RNA localization sequences. In addition, the enzymatic assay was more rapid and convenient than in situ hybridization.

Using the spatial expression characteristics of these chimeric gene products, a 54-nt zipcode was mapped to the 3′UTR of β-actin just proximal to the coding region. A series of 3′-deletions and subcloned fragments of the β-actin cDNA were evaluated for their ability to target β-galactosidase activity to the leading edge of transfected CEFs (Fig. 2). A significant 5.8-fold (32.6%/5.6%) increase in localization over the vector was found using the full-length β-actin insert fused to β-galactosidase ($p \leq 0.0002$). Equally significant increases in localization were found with two 3′-exonuclease deletion constructions, construct B with 458 of 591 nt of 3′UTR deleted and construct C with 536 nt deleted. A 483-bp fragment containing 43 nt of coding sequence through 440 nt of the 3′UTR (construct D) also localized as well (6.9-fold). In construct C, all but the first 54 nt of the 591 nt 3′UTR were removed from the full-length β-actin cDNA; further deletion of the entire 3′UTR plus 20 nt of coding region (construct E) resulted in a level of activity indistinguishable from the vector control ($p = 1.0$). When evaluated separately, the last 20 nt of β-actin coding region and its entire 3′UTR (construct F) was sufficient to target β-galactosidase activity to the peripheral cytoplasm as well as the full-length actin cDNA and highly significant relative to the vector control ($p \leq 0.0002$). Overall, these results indicated that the zipcode existed proximal to the stop codon.

Three synthetic oligonucleotides were evaluated: the putative zipcode within the first 54 nt of the 3′UTR including the stop codon (construct G), and sequences flanking this putative zipcode in the coding region (construct H) and in the 3′UTR (construct I). Peripheral localization activity directed by construct G was comparable to the full-length cDNA ($p \leq 0.0002$). The activities of the flanking regions (constructs H and I) were not significantly different from either the vector alone or the 5′UTR plus coding region ($p \geq 0.99$ in all cases). Therefore, the first 54 nt of the β-actin 3′UTR was sufficient to target a heterologous mRNA to the peripheral cytoplasm.

To determine if the zipcode was the sole element necessary for localization, it was deleted from full-length β-actin cDNA (construct J). Its removal significantly reduced, but did not eliminate, localization activity relative to the full-length insert. Activity was contained within the remaining 3′UTR fragment (construct K) and was significant relative to the vector ($p \leq 0.24$). Within that segment, homologies with the 54-nt zipcode were evident in a 43-nt sequence (construct L) which contained half the localization activity of the 54-nt zipcode (17 vs 33%) and was significant relative to the vector ($p < 0.79$).

To ascertain whether the 54- and 43-nt segments were the

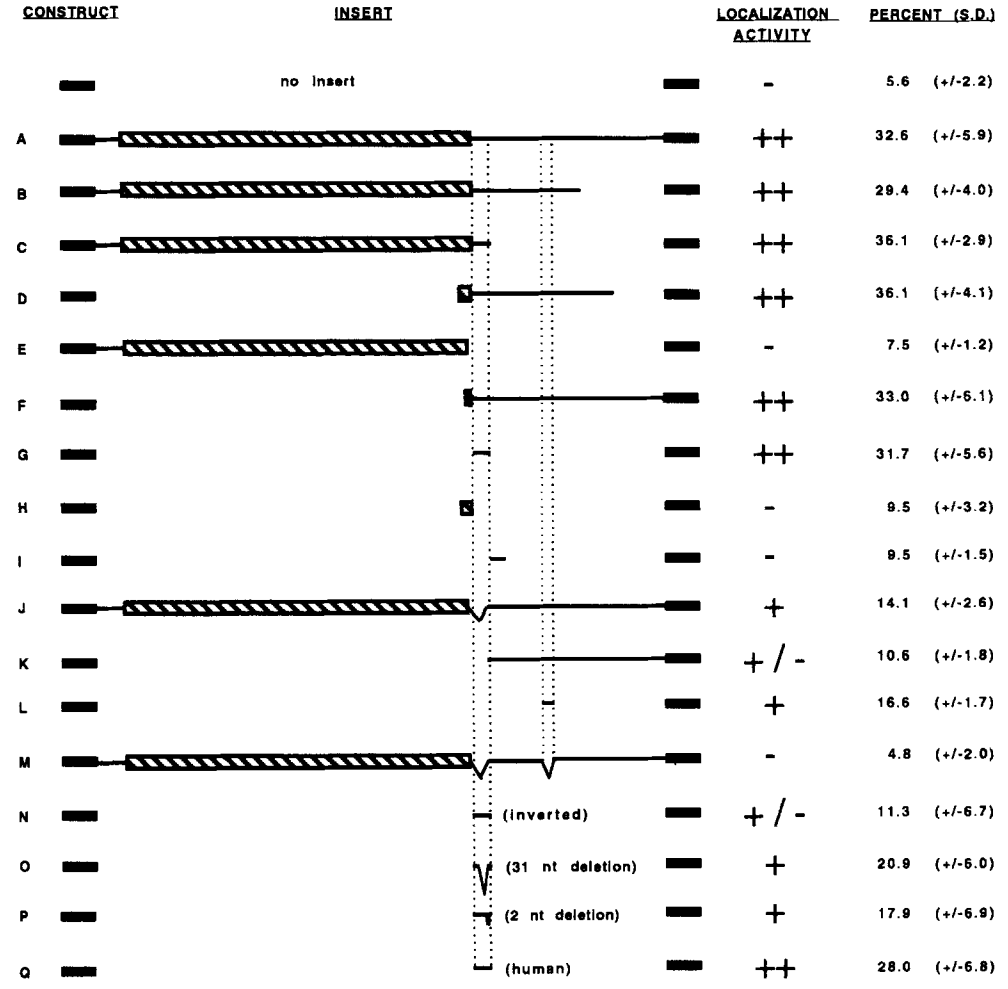

Figure 2. Localization determinants mapped to a 54-nt and a 43-nt segment of the β-actin 3′UTR. Schematic of a series of restricted β-actin cDNA sequences inserted into the RSVβgal plasmid 3′ polylinker. Designated schematically are vector polylinker sequences (*solid filled box*), β-actin coding sequences (*diagonally hatched box*), and β-actin 3′UTR sequences (*solid line*). Each construct (*A–N*) was evaluated in 3–20 independent experiments with 300 to several thousand transfected (blue) cells counted per experiment. Transfectants were scored as localized or nonlocalized based on whether the cytoplasmic distribution of blue staining was peripheral or nonlocalized. The percent of transfectants with peripheral blue staining was calculated for each experiment. The activity was summarized for each construct based on statistical significance: ++ >27%; + 14–28%; +/− 10–14%; and − <10%. The position of the 54-nt zipcode and 43-nt segments within the 3′UTR are indicated with vertical dotted lines.

sole localization determinants, both were deleted from the full-length insert (construct M). This double mutant (construct M) was incapable of localizing β-galactosidase, and its activity was indistinguishable from the vector alone. Therefore, only these two segments function to target β-actin mRNA to the peripheral cytoplasm. Because the first 54 nt of the 3′UTR contained activity comparable to the entire β-actin cDNA, we refer to it as the "peripheral RNA zipcode". The 43-nt segment with submaximal activity and homology to the peripheral RNA zipcode is composed of "zipcode elements."

To test orientation dependence, the 54-nt zipcode was inverted (construct N). Inversion of the zipcode reduced the percent localized from 33 to 11% of the transfectants, a level which was not significantly different from the vector ($p \geq 0.81$). To address the question of position dependence, the zipcode was inserted into the reporter 5′UTR. Because of a shift in the reading frame, β-galactosidase was not translated when the zipcode (which contains an initiation codon) was inserted into the 5′UTR in the normal orientation. Localization activity in this case was evaluated by in situ hybridization. Quantitation of transfectants showed weak but significant localization activity (15%), relative to the vector alone, when inserted into the 5′UTR. Possibly, insertion of the zipcode sequences upstream of the LacZ coding region may inhibit ribosome-scanning or zipcode-binding protein function, or both. In either case, it would appear from these results that zipcode function orientation-dependent and position-dependent within the mRNA.

Fine Structure of the Zipcode

Sequence homology between the 54- and 43-nt segments might be expected to identify the minimal zipcode sequence. Two motifs, GGACT and AATGC, are present in both segments (Fig. 3). The GGACT motif occurs at the 5′-end and the AATGC motif occurs at the 3′-end of the 54-nt zipcode. To evaluate whether the sequences between these motifs function in localization, positions 10 through 40 in the 54-nt zipcode were deleted (construct O). Deletion of those sequences reduced localization activity (20.9%), comparable to the 43-nt segment ($p = 1.0$), but significantly different from the vector alone ($p \leq 0.095$). This suggested that the sequences between position 10 and 40 are important for enhancing localization. Possibly two ACACCC motifs removed from the 54-nt segment (construct O) contribute to its activity. A two base deletion of the 54-nt zipcode (construct P) which removed the A and T residues adjacent the AATGC motif was tested. This resulted in reduced localization activity (16%), significantly different from the 54-nt zipcode ($p \leq 0.002$), indicating the importance of the 3′-motif sequence for localization.

To test the contribution of the two motifs, independently, each was synthesized as a cassette and evaluated. Remarkably, both the GGACT motif (inserted as TAAACCGGACTGT) and the AATGC motif (inserted as AACCCATAAATGC) were each found to contain weak localization activity (15.2 ± 2.3% and 19.3 ± 7.2%, respectively). Their activities were not significantly different from each other or the combination of the two together in construct O ($p = 1.0$ in all cases). However, localization activity of the 5′ motif GGACT was slightly less significant than the 3′ motif relative to the vector alone ($p \leq 0.129$ and $p \leq 0.002$, respectively). The size or number of zipcode motifs may also be important for maximal localization. To determine whether these motifs inserted as tandem repeats would function more efficiently, the vector containing three copies of the GGACT motif, in the context of the first 10 nt of the 3′UTR and stop codon, and the vector containing four copies of the AATGC motif, in the context of the last 13 nt of the zipcode, were evaluated separately. Both constructs bearing tandem copies of each motif showed enhanced localization activity. Four copies of the 3′ motif (AATGC) localized almost as effectively as the entire intact zipcode (27.5 ± 1.6%), while three copies of the 5′ motif (GGACT) had somewhat less activity (20.7 ± 8.9%). These data indicated that the elements which comprise the entire 54-nt zipcode each contain submaximal localization activity. The weak localization activity of at least one motif in the zipcode can substitute for the activity of the entire zipcode when multimerized. The high A/C content in the 54-nt zipcode, contained within both 5′ and 3′ motifs, appearing as AAACC, ACACCC, or AACAAA may play a part in the mechanism of β-actin mRNA localization. The zipcode, therefore, appears to be composed of several minimal motifs, each of which adds proportionately to the localization.

Conservation of Zipcodes

Further insight into essential sequences required for zipcode function was revealed by comparing the chicken zipcode with the homologous region of the human β-actin cDNA. The mechanism of RNA localization, and hence the zipcode sequences, would be expected to be conserved between

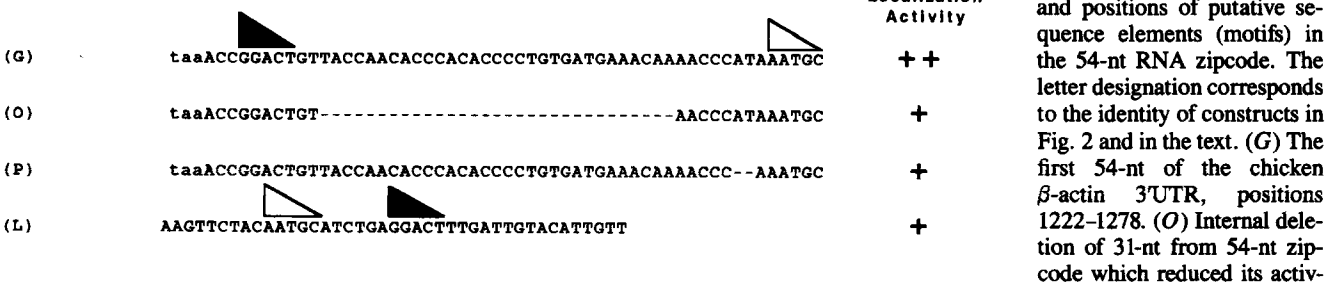

Figure 3. Nucleotide sequence and positions of putative sequence elements (motifs) in the 54-nt RNA zipcode. The letter designation corresponds to the identity of constructs in Fig. 2 and in the text. (*G*) The first 54-nt of the chicken β-actin 3′UTR, positions 1222–1278. (*O*) Internal deletion of 31-nt from 54-nt zipcode which reduced its activity from ++ to +. (*P*) Two base internal deletion which reduced its activity from ++ to +. (*L*) Chicken β-actin 43-nt zipcode with + activity (positions 1412-1452). Shared sequence motifs are oriented by wedge-shaped arrowheads over each sequence, a 5′ motif by a solid wedge and a 3′ motif with an open wedge. Note the order of the two motifs are reversed in the 43-nt segment vs the 54-nt zipcode.

chicken and human β-actin since primary cultures of human fibroblasts also localize β-actin mRNA to the leading lamellae (Kislauskis, E.H., unpublished data). A strong selective pressure to retain these functional elements would explain regions of high conservation among the 3′-untranslated reions of vertebrate β-actin genes (Ponte et al., 1983; Yaffe et al., 1985). More conservation occurs in the 5′ region of the 3′UTR, where the zipcodes reside. A comparison of the first 54 nt of 3′UTR of the chicken and the human revealed 65% identity.

```
(ch) ACCGGACTGTTACCAACACCC---ACACCCCTGTGATGAAACAAAACCCATAAA-TGC
     |||||| | || |   |  |||||| | |  ||| |||||||  |||  |||
(hu) G-CGGACTATGACTTAGTTGCGTTACACCC-TTTCTTGA--CAAAACC--TAACTTGC
```

Consistent with a conservation of nucleotide sequence between β-actin 3′UTR regions, we found that zipcode function was similarly conserved. The first 54 nt of the human β-actin 3′UTR (construct Q) localized β-galactosidase in chicken cells quantitatively indistinguishable from the homologous segment of the chicken 3′UTR (28%). This suggests that the cellular mechanism of zipcode function and specificity has been conserved evolutionarily. An alignment of the chicken and human zipcode sequences revealed considerable homology particularly at the 3′ end of the 54-nt segment where eight consecutive nucleotides occur in a conserved region of 13/16 (81% identity). This supports and confirms the importance of this element in localizing the mRNA as was shown with the genetic chimeras. In particular, the AATGC motif, described above is represented in the human sequence as AACTTGC. It is possible that these conserved sequences represent elements of the zipcode which are essential for maximal localization activity. A complementary pair of oligonucleotides were synthesized, fused to LacZ, and tested in CEFs (construct Q). Because this construct functioned as well in chicken cells as the chicken zipcode (28%), it validated the conservation of the RNA zipcode mechanism. Furthermore, conserved sequences between these diverse species are likely to be required for the mechanism. Alignment of these sequences showed short stretches throughout the zipcode, some as long as 8 nt. Therefore, this confirms the conclusion that the zipcode appears to be composed of multiple dispersed elements which act in concert to provide maximal activity.

Functional Properties of the β-Actin RNA Zipcode

To confirm the role of the zipcode to localize endogenous actin mRNA, phosphorothioate-modified oligonucleotides were used as antisense to inhibit zipcode function. The effects of these modified oligonucleotides (18-mers) on actin mRNA localization and cell phenotype was assessed after a 12-h treatment. The positions and orientations relative to the β-actin RNA zipcode are diagrammed schematically (Fig. 4). Treatment with antisense oligonucleotides corresponding to zipcode sequences resulted in a suppression of β-actin mRNA localization relative to untreated CEFs, while a sequence flanking the zipcode and a sense sequence had no effect. In particular, oligo C (the 3′ end of the zipcode) reduced the percent of CEFs with a peripheral distribution of actin mRNA to 21% of control. Antisense oligonucleotides A and B (the 5′ two-thirds) were less effective (33 and 37% of control, respectively). Similarly, oligonucleotides complementary to the 5′ half (oligo E) and 3′ half (oligo F) of the 43-nt RNA zipcode element reduced localized actin mRNA (51 and 29%, respectively). The mechanism may involve sequence homologues between the zipcode elements. In striking contrast, neither the 3′UTR sequences flanking the 54-nt segment (oligo D) nor the sense strand of the most effective inhibitory probe (oligo C+) reduced actin mRNA localization relative to control, (91 and 98%, respectively). These data add strong support to the role of the RNA zipcode in endogenous β-actin mRNA localization to the cell periphery.

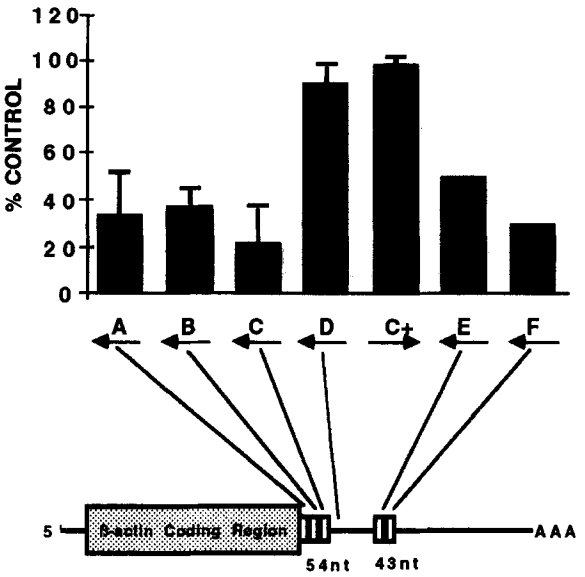

Figure 4. Quantitation of the effects of antisense oligonucleotide treatment on endogenous β-actin mRNA localization. Effects of six antisense oligonucleotides (*A–F*) and one sense oligonucleotide (*C+*) on endogenous actin mRNA localization in CEFs relative to a control (nontreated) culture. Each oligonucleotide is depicted schematically, corresponding to portions of the 54-nt RNA zipcode and flanking sequences. The percent of CEFs with localized endogenous β-actin mRNA relative to untreated cultures was evaluated by in situ hybridization after a 12-h treatment with 8 μM concentration of each antisense oligonucleotide. Oligonucleotides complementary to RNA zipcode sequences significantly delocalized endogenous β-actin mRNA while control oligonucleotides had virtually no effect.

The effects of antisense treatment on actin mRNA distribution are illustrated (Fig. 5, *left panels*). A normal peripheral

Figure 5. Effects of antisense treatments on endogenous β-actin mRNA localization and the actin cytoskeleton. CEFs treated for 12 h with various phosphorothioate oligonucleotides were processed to detect endogenous actin mRNA localization by in situ hybridization (*left panels*) or stained with FITC-phalloidin and DAPI (*right panels*). (*A* and *B*) Antizipcode oligonucleotide (*Oligo C*); (*C* and *D*) sense strand of the antizipcode oligonucleotide (*Oligo C+*); (*E* and *F*) antisense oligonucleotide to the flanking region (*Oligo D*); and (*G* and *H*) control cells without antisense treatment. Note that control CEFs and those treated with oligo C+ or D showed localized actin mRNA at the leading lamellae and polarized cell phenotypes, with parallel actin filaments oriented toward the lamellipodia. In contrast, CEFs treated with oligo C showed nonlocalized actin RNA, nonpolarized phenotypes, and actin stress fibers oriented in many directions. Bars: (*left panels*, *A*, *C*, *E*, and *G*) 30 μm; (*right panels*, *B*, *D*, *F*, and *H*) 20 μm.

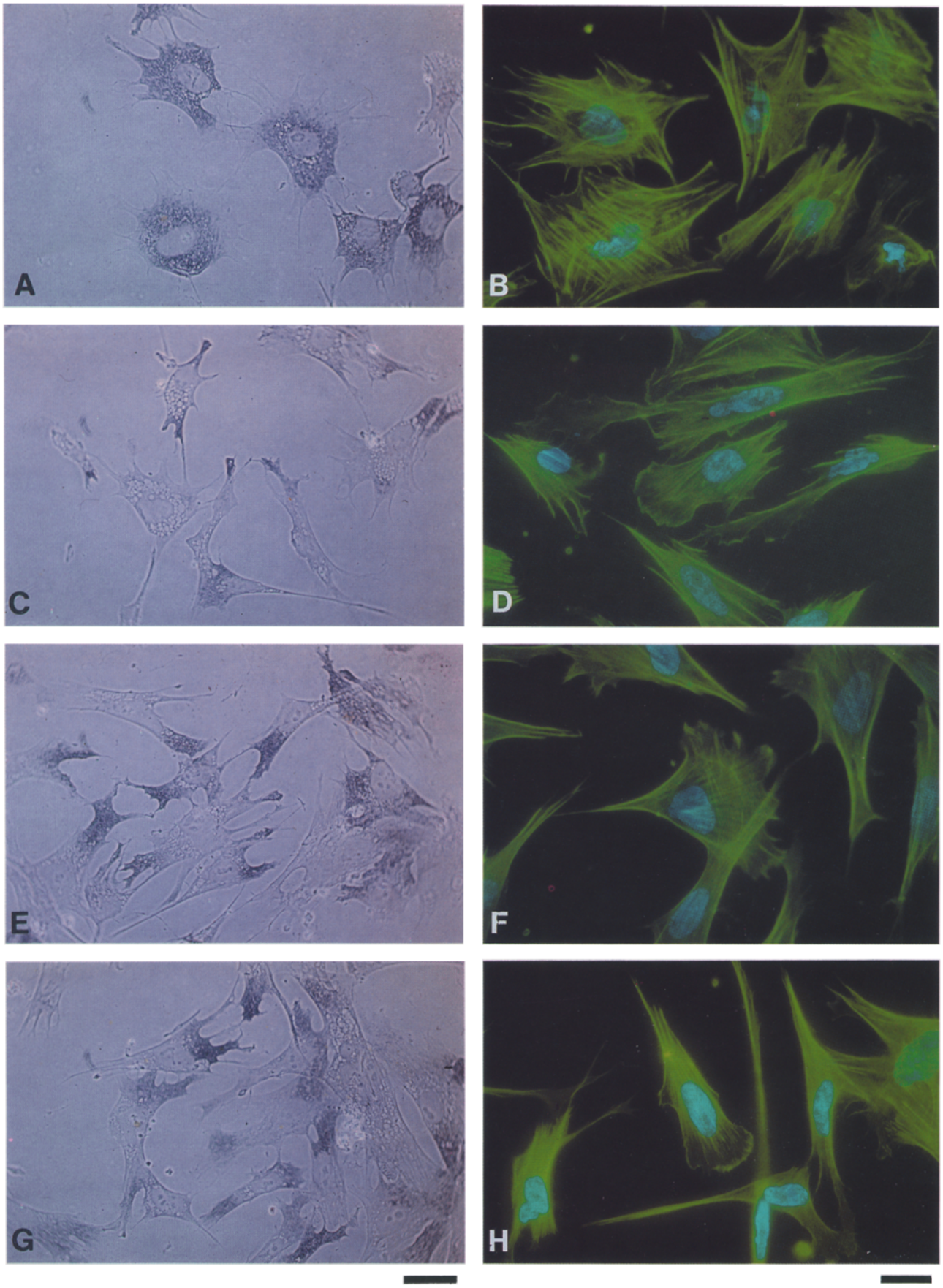
A
B
C
D
E
F
G
H

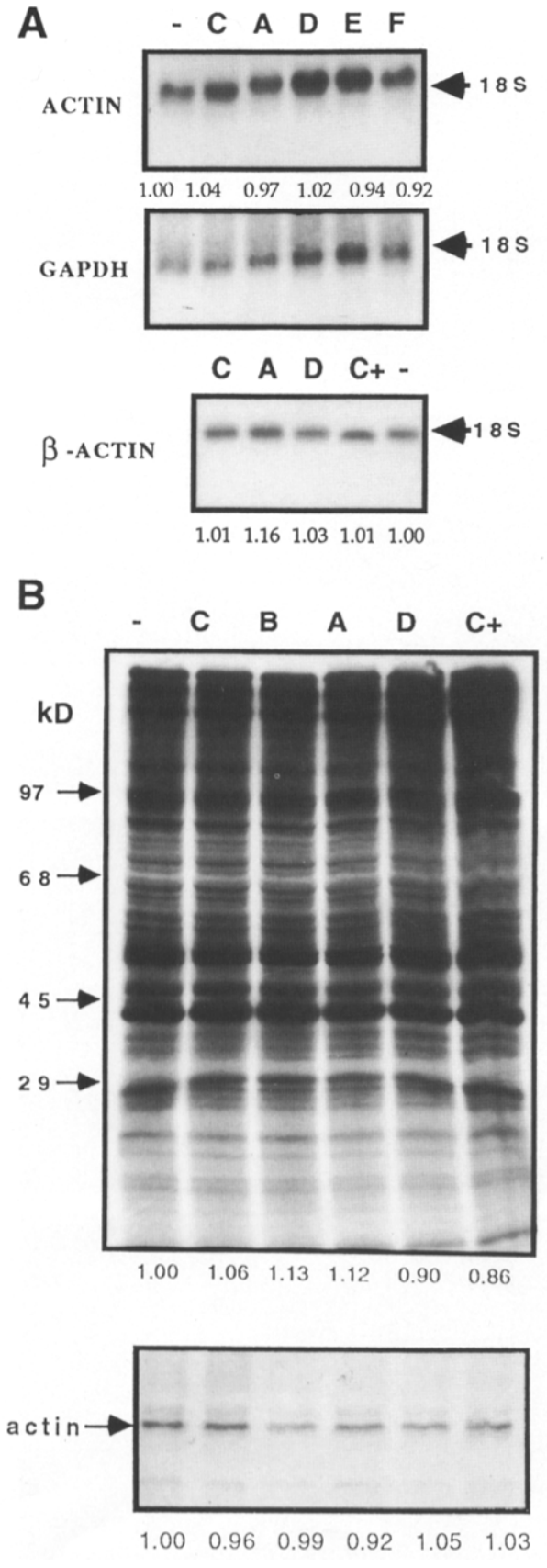

Figure 6. Antisense oligonucleotides do not destabilize steady state β-actin mRNA levels, or suppress actin protein synthesis. (*A*) Northern blot analyses of total RNA were extracted from control cells (*dash mark*) and cells treated for 12 h (three treatments, of 4 h each) with 8 μM oligo *C*, *A*, *D*, *E*, or *F* and probed with β-actin cDNA (*upper panel*) and GAPDH cDNA (*middle panel*). The ratio of ~1.8 kb actin mRNA signal to ~1.3 kb GAPDH mRNA in each case shows no change in actin mRNA levels resulting from the antisense treatments. Hybridization to β-actin 3′UTR sequences (*lower panel*) showed comparable results relative to ethidium-stained 18 S ribosomal RNA. No indication of antisense-induced RNAse H activity was evident in the size distribution of actin mRNA signal in the upper and lower panels. Arrows indicate the position of 18S ribosomal RNA. (*B*) SDS-PAGE gel electrophoresis of total-labeled proteins extracted from control cells and cells treated for 12 h with 8 μM oligonucleotides *A–D* and *C+*, after a 30-min pulse with [^{35}S]methionine. The relative ratio of actin (43 kD) to the 29 kD band is shown (*upper panel*). Quantitation relative to total protein of amounts of β-actin after immunoprecipitation with a β-actin-specific antibody is shown (*lower panel*). The results of both analyses indicate no appreciable effect on β-actin (43 kD) protein synthesis.

distribution of actin mRNA and characteristic polarized phenotype were maintained in untreated CEFs (control) and CEFs treated with oligo C+ (zipcode sense) and oligo D (flanking the zipcode). In contrast, CEFs treated with oligo C (the 3′ end of the zipcode, *upper left panel*) showed a non-localized, homogeneous distribution of actin mRNA and a change to a nonpolarized morphology. In addition, cells treated with oligo C became stellate in shape with collapsed lamellae and were less well spread, suggesting a reduced adhesion to the substrate. These data imply that the asymmetric distribution of actin mRNA localization may be reflected in a concomitant structural asymmetry, most likely of the actin cytoskeleton. To assess the distribution of actin filaments after incubation with the antisense oligonucleotides, CEFs were stained with phalloidin (Fig. 5; *right panels*). Unlike control cells and cells treated with oligo D, where actin staining is concentrated within the leading edge, and stress fibers are polarized toward the leading lamellae, CEFs treated with oligo C showed no leading edge and little actin staining at the periphery; the actin filament system was organized perinuclearly. Thus, the actin cytoskeleton reorganized after treatment with antizipcode oligo C, but not with the sense strand (oligo C+), or a flanking sequence (oligo D).

Delocalization of the mRNA by the antisense treatment may have resulted from a disruption of a specific aspect of the localization pathway, such as transport or anchoring. Alternatively, the steady state level or integrity of actin mRNA may have been affected by the treatment. To address the latter issue, Northern blot analysis was performed on total RNA extract from CEFs after each antisense oligonucleotide treatment (Fig. 6 *A*). Actin mRNA levels were compared directly to an internal standard, GAPDH mRNA. No substantial change in steady state levels of actin mRNA was observed (±15%) relative to the GAPDH. Moreover, the Northern analysis revealed no change in the size distribution of actin mRNA after incubation with the antisense oligonucleotides which indicate that RNAse H–mediated degradation did not occur. Therefore, the inhibition of actin mRNA localization cannot be explained by an effect on mRNA stability or integrity. These conclusions were confirmed with a separate Northern blot of RNA from similarly treated CEFs probed with β-actin 3′UTR sequences showing no change in β-actin mRNA quantity or quality.

There are at least two mechanisms by which antizipcode oligonucleotides could affect actin expression, and, thereby, cell phenotype. First, inappropriately localized actin mRNA may suppress actin protein synthesis. Over the 12-h treatment, this could deplete the cellular pool of G-actin. Alternatively, nonlocalized actin mRNA could affect the site of actin protein synthesis, and consequently influence sites of actin polymerization. To distinguish between these possibilities, CEFs were treated with each oligonucleotide for 12 h, pulse-labeled with [^{35}S]methionine, and extracted. No change in total cellular actin synthesis (<14%) relative to a 29-kD band on the autoradiogram was observed among the various antisense probes (Fig. 6 *B*). To address the question of whether expression of the β-actin isoform was specifically affected by this treatment, equal counts of the same extracts were immunoprecipitated using a β-actin specific antibody. Quantitation of the 43-kD β-actin band in each case relative to the untreated control extract indicated no significant effect in β-actin synthesis. Therefore, the striking change in cell phenotype that resulted from exposure to an antisense oligonucleotide (oligo C, Fig. 5, *A* and *B*) could not be due to its effect on actin synthesis per se. Rather, we conclude that the consequence of treatment with antizipcode oligonucleotides on cell phenotype resulted from a change in the site of β-actin synthesis, and, hence, the site of actin concentration within the cell. This data supports the hypothesis that the RNA zipcode directs β-actin mRNA to the cell periphery where the protein synthetic apparatus can provide a compartmentalized source of G-actin to facilitate the assembly of actin filaments involved in the maintenance of cell structure, polarity, and motility.

Discussion

Three approaches were used to define *cis*-acting sequences in the β-actin 3′-UTR that are essential for peripheral mRNA localization. First, transiently expressed LacZ/β-actin RNA chimeras enabled identification of two short segments of 3′UTR capable of directing β-galactosidase activity to the peripheral cytoplasm. The localization activity resided in a principal RNA zipcode within the first 54 nt, and in a related but weaker secondary 43 nt sequence further downstream. Second, the homologous region of the human β-actin 3′UTR acted effectively as a zipcode in chicken cells. Conserved sequence motifs between these divergent species may therefore be functionally important. Third, the functional importance of the zipcode was confirmed using antisense oligonucleotides to the sequences predicted by chimeric genes to be essential for actin mRNA localization. Oligonucleotides complementary to portions of the 54-nt zipcode or the 43-nt segment, delocalized endogenous β-actin mRNA and altered cell morphology. Our antizipcode oligonucleotides do not appear to destabilize mRNA nor do they suppress the synthesis of actin protein relative to control oligonucleotides. We conclude that the RNA zipcode is critical to the mechanism of actin mRNA localization and for the organization of the actin cytoskeleton.

This use of antisense technology to modulate the distribution of mRNA, rather than for the purposes of inhibition of gene expression, represents a novel application. Whether other mRNAs with identical peripheral RNA zipcode motifs were affected by this antisense treatment is unknown. Functionally related mRNAs could determine cell polarity or morphology by spatial coordination of their sites of protein synthesis. Hence, interaction between cognate proteins would be facilitated by increased concentrations within the correct cytoplasmic compartment. A comparison of the β-actin localization sequence to a database (Genetics Computer Group, Madison, WI) has revealed sequence homologies with mRNAs encoding actin-associated proteins, including fibrin, villin, and members of the Marcks family. Whether these homologies are zipcodes remains to be determined. However, Northern blot analysis using the oligonucleotide probes indicates that hybridization is β-actin mRNA-specific (data not shown).

In general, RNA localization signals have been mapped to the 3′ ends of mRNAs. For instance, sequences involved in the anterior localization of *bicoid* mRNA in *Drosophila* oocytes, originally mapped by genetic complementation to a 625-nt 3′UTR segment (Macdonald and Struhl, 1988), have recently been refined to several smaller regions, including a 50-nt segment necessary in the early stages of localization, BLE1 (Macdonald et al., 1993). Other *Drosophila* 3′UTR localization signals include an anterior localization signal in the zygotic K10 gene restricted to a ~1.4-kb 3′ segment (Cheung et al., 1992). Posterior localization signals have been found within the ~1.7-kb segment of the maternal mRNA coding for *nanos* (Gavis and Lehmann, 1992), the ~1.1-kb 3′UTR of *oskar* (Kim-Ha et al., 1993), and two closely apposed segments of 94 and 87 nt within the *cyclin B* (Dalby and Glover, 1993). In blastoderm embryos, apical localization signals have been identified on zygotic pair-rule transcripts with the shortest occurring within the last 124 nt of the *even-skipped* gene (Davis and Ish-Horowicz, 1992). In *Xenopus* oocytes, a vegetal pole localization signal has been restricted to a 340-nt region of the maternal *vg-1* mRNA (Mowry and Melton, 1992). To resolve details of the mechanism of RNA localization in each case will require more accurately delimited zipcode sequences.

Our analyses indicate that functional components of the β-actin mRNA zipcode are quite diminutive in size. Deletions within the 54-nt sequence reduced but did not eliminate localization activity (data not shown). These observations, and the work of others, indicate that RNA localization signals have size constraints and are multicomponent in their organization. The potential of 3′UTR sequences to form multiple stem-loops (e.g., *Drosophila* Bicoid genes) has suggested that localization may involve RNA secondary structure (Macdonald, 1990). Such a model would predict that separate 3′ elements hybridize to form a secondary structure necessary to interact with the localization machinery. Both *bicoid* and *oskar* mRNA localization sequences appear to be composed of multiple interspersed segments which could function at different steps in the process (Kim-Ha et al., 1993; Macdonald et al., 1993). The identification of at least two localization elements in the β-actin mRNA supports the principle of redundancy of zipcode elements in the 3′UTR, but the sequences show little, if any, complementarity, and do not support the role of secondary structure in RNA localization. This is unusual as most functional RNA elements form secondary structure (Klausner et al., 1993).

In some cases, differential RNA localization might be explained by a translational control mechanism. For instance, repression of translation of two morphogens, *bicoid* and

hunchback, requires *nanos* (*nos*) protein, occurs through a small 3'UTR sequence called *nos*-responsive element (NRE), which may act to destabilize NRE containing RNAs (Wharton and Struhl, 1991). The NRE appears to be necessary for the translational control but not localization of cyclin B mRNA at the posterior pole (Dalby and Glover, 1993). A distinction between localization determinants and NREs also remains unclear for the *C. elegans* glp-1 gene. Expression of GLP-1 protein is spatially and temporally regulated, is localized to anterior blastomeres, and appears to be important for the specification of several anterior cell fates. Recently, NRE-like motifs have been identified within a 61-nt segment of glp-1 3'-untranslated region critical for the spatial control GLP-1 expression, and not within the adjacent uridine-rich 125 nt critical for its temporal control (Evans et al., 1994). The possibility that the β-actin RNA zipcode functions in this manner, as a temporal control region, appears unlikely based on the fact that β-galactosidase expression was not appreciably reduced or increased between the various constructs, nor were there any significant differences in transfection efficiency of the various constructs. Thus, there can be no gross differences in reporter RNA stability. For similar reasons, translational efficiency of the β-galactosidase mRNA chimeras does not appear to be a factor in localization.

That components of the mechanism of mRNA localization may be highly conserved throughout evolution is not entirely surprising. The mechanism of mRNA localization is dependent on cytoskeletal filaments (Pokrywka and Stephenson, 1991; Sundell and Singer, 1991; Theurkauf et al., 1992; Yisraeli et al., 1990). Actin and tubulin, themselves, are highly conserved evolutionarily. It is possible that homologous elements within zipcodes form binding sites for highly conserved proteins involved in mRNA transport or the anchoring. Factors which recognize conserved mRNA sequences as well as conserved cytoskeletal proteins may include some of the well-known cytoskeletal-associated proteins. These cytoskeletal and cytoskeletal-associated proteins are highly conserved even in yeast (Drubin, 1990; Drubin et al., 1992) and would be expected to be involved in some part of the mechanism of RNA localization including sequence recognition, protein binding, and ultimately transport and anchoring. Further information will require biochemical and genetic characterization of cellular factors which bind specifically to the zipcode sequences.

In motile cells, such as CEFs and myoblasts, β-actin isoform and its mRNA predominates in the periphery of the cell, compared to other actin isoforms which are perinuclear (Hill and Gunning, 1993; Hoock et al., 1991; Kislauskis et al., 1993). Cell morphology may result from the differences in where each isoform is synthesized. For instance, deletion of the 3'UTR of γ-actin results in changes in myoblast morphology (Lloyd and Gunning, 1993). Our data suggest a relationship between β-actin mRNA localization and the disposition of actin filaments in these motile cells. The consequence of delocalizing β-actin mRNA therefore appears to be a disruption in the asymmetric supply of β-actin within the leading lamellae, possibly essential for the maintenance of cell polarity.

Finally, the work further supports the role of the 3'UTR as a repository of regulatory elements (Jackson, 1993). RNA zipcodes can be included as one of multiple *cis*-regulatory signals in the 3'UTR, including those that control translation (Peltz and Jacobson, 1992) or mRNA stability (Hale et al., 1992). This work also provides a mechanistic basis for the significance of 3'UTR sequences in determining cell differentiation and behavior (Rastinejad and Blau, 1993; Rastinejad et al., 1993). RNA zipcodes add another dimension to these controls of gene expression in the cytoplasm.

We thank our colleagues Drs. J. M. Mathys, A. Ross, and M. Rosbash, and A. Jacobson for their editorial comments; Zhi-wen Zhang for her technical assistance early in the project; and Dr. J. Bulinski for donating the actin antibodies used in these experiments.

A portion of this work was presented at the American Society of Cell Biology, Kislauskis, E. H., and R. H. Singer. 1991. *J. Cell Biol* 115:158a. This work was supported by National Institutes of Health grants AR41480 and HD18066 to R. H. Singer, and a post-doctoral fellowship from the Muscular Dystrophy Association to E. H. Kislauskis.

Received for publication 20 April 1994 and in revised form 12 July 1994.

References

Bretcher, A. 1991. Microfilament structure and function in the cortical cytoskeleton. *Annu. Rev. Cell Res.* 7:337–374.

Carlier, M. 1991. Actin: protein structure and filament dynamics. *J. Biol. Chem.* 266:1–4.

Cheung, H., T. L. Serano, and R. S. Cohen. 1992. Evidence for a highly selective RNA transport system and its role in establishing the dorsoventral axis of the *Drosophila* egg. *Development.* 114:653–661.

Cleveland, D. W., M. A. Lopata, R. J. MacDonald, N. J. Cowan, W. J. Rutter, and M. W. Kirscher. 1980. Number and evolutionary conservation of α- and β-tubulin and cytoplasmic β- and γ-actin genes using specific cloned cDNA probes. *Cell.* 20:95–105.

Cooper, J. A. 1991. The role of actin polymerization in cell motility. *Annu. Rev. Physiol.* 53:585–605.

Dalby, B., and D. M. Glover. 1993. Discrete sequence elements control posterior pole accumulation and translational repression of maternal cyclin B RNA in *Drosophila. EMBO (Eur. Mol. Biol. Organ.) J.* 12:1219–1227.

Davis, I., and D. Ish-Horowicz. 1992. Apical localization of pair-rule transcripts requires 3' sequences and limits protein diffusion in the Drosophila blastoderm embryo. *Cell.* 67:927–940.

Drubin, D. G. 1990. Actin and actin-binding proteins in yeast. *Cell Motil. Cytoskeleton.* 15:7–11.

Drubin, D. G., Z. Zhu, J. Mullholland, and D. Botstein. 1992. Homology of yeast actin binding proteins to signal transduction proteins and myosin-I. *Nature (Lond.).* 343:288–290.

Evans, T. C., S. L. Crittenden, V. Kodoyianni, and J. Kimble. 1994. Translational control of maternal *glp-1* mRNA establishes an asymmetry in the C. elegans embryo. *Cell.* 77:183–194.

Farwell, A. P., R. M. Lynch, W. O. Okulicz, A. M. Comi, and J. L. Leonard. 1990. The actin cytoskeleton mediates the hormonally regulated translocation of type II iodothyrodinine 5'-deiodinase in astrocytes. *J. Biol. Chem.* 265:18546–18553.

Gavis, E. R., and R. Lehmann. 1992. Localization of *nanos* RNA controls embryonic polarity. *Cell.* 71:301–313.

Hale, D. L., T. A. Roualt, C. K. Tang, L. Chin, H. B. Harford, and R. D. Klausner. 1992. Reciprocal control of RNA-binding and aconitase activity in the regulation of the iron-responsive element binding protein: role of the iron-sulfur cluster. *Proc. Natl. Acad. Sci. USA.* 89:7536–7540.

Hesketh, J., and I. F. Pryme. 1991. Interaction between mRNA, ribosomes and the cytoskeleton. *Biochem. J.* 277:1–10.

Hill, M. A., and P. Gunning. 1993. Beta and gamma actin mRNAs are differentially located within myoblasts. *J. Cell Biol.* 122:825–832.

Hoock, T. C., P. M. Newcomb, and I. M. Herman. 1991. β actin and its mRNA are localized at the plasma membrane and the regions of moving cytoplasm during the cellular response to injury. *J. Cell Biol.* 112:653–664.

Hunt, A. N., I. C. Normand, and A. D. Postle. 1990. CTP: cholinephosphate cytidylyltransferase in humans and rat lung: association in vitro with cytoskeletal actin. *Biochim. Biophys. Acta.* 1043:19–26.

Jackson, R. J. 1993. Cytoplasmic regulation of mRNA function: the importance of the 3' untranslated region. *Cell.* 74:9–14.

Kim-Ha, J., P. J. Webster, J. L. Smith, and P. M. Macdonald. 1993. Multiple RNA regulatory elements mediate distinct steps in localization of *oskar* mRNA. *Development.* 119:169–178.

Kislauskis, E. H., Z. Li, R. H. Singer, and K. L. Taneja. 1993. Isoform-specific 3'-untranslated sequences sort α-cardiac and β-cytoplasmic actin messenger RNAs to different cytoplasmic compartments. *J. Cell Biol.* 123:165–172.

Klausner, R. D., T. A. Rouault, and J. B. Harford. 1993. Regulating the fate of mRNA: the control of cellular iron metabolism. *Cell.* 72:19–28.

Knull, H. R., and J. L. Walsh. 1992. Association of glycolytic enzymes with the cytoskeleton. *Curr. Top. Cell. Regul.* 33:15–30.

Kuznetsov, S. A., G. M. Langford, and D. G. Weiss. 1992. Actin-dependent organelle movement in squid axoplasm. *Nature (Lond.)*. 356:722–725.

Latham, V. M., E. H. Kislauskis, R. H. Singer, and A. F. Ross. 1994. β-actin mRNA localization is regulated by signal transduction mechanisms. *J. Cell Biol.* 127:1211–1219.

Lawrence, J. B., and R. H. Singer. 1986. Intracellular localization of messenger RNA for cytoskeletal proteins. *Cell.* 45:407–415.

Lawrence, J. B., K. L. Taneja, and R. H. Singer. 1989. Temporal resolution and sequential expression of muscle-specific genes by *in situ* hybridization. *Dev. Biol.* 133:235–246.

Levitt, J., S. Ng, U. Aebi, M. Varma, G. Latter, S. Burbeck, and P. Gunning. 1987. Expression of transfected mutant β-actin genes: alterations of cell morphology and evidence for autoregulation of actin pools. *Mol. Cell. Biol.* 7:2457–2466.

Lloyd, C., and P. Gunning. 1993. Noncoding regions of the γ-actin gene influence the impact of the gene on myoblast morphology. *J. Cell Biol.* 121:73–82.

Macdonald, P. M. 1990. *bicoid* mRNA localization signal: phylogenetic conservation of function and RNA secondary structure. *Development.* 110: 161–167.

Macdonald, P. M., and G. Struhl. 1988. Cis-acting sequences responsible for anterior localization of *bicoid* mRNA in *Drosophila* embryos. *Nature (Lond.)*. 336:595–598.

Macdonald, P. M., K. Kerr, J. L. Smith, and A. Leask. 1993. RNA regulatory element BLE1 directs the first step of *bicoid* mRNA localization. *Development.* 118:1233–1243.

Mowry, K. L., and D. A. Melton. 1992. Vegetal messenger RNA localization directed by a 340-nt RNA sequence element in *Xenopus* oocytes. *Science (Wash. DC).* 255:991–994.

Negrutskii, B. S., and M. P. Deutscher. 1991. Channelling of aminoacyl-tRNA for protein synthesis *in vivo*. *Proc. Natl. Acad. Sci. USA.* 88:4991–4995.

Otey, C. A., M. H. Kalnoski, and J. C. Bulinski. 1987. Identification and quantitation of actin isoforms in vertebrate cells and tissues. *J. Cell. Biochem.* 34:113–124.

Peltz, S. W., and A. Jacobson. 1992. mRNA stability: in trans-it. *Curr. Opin. Cell Biol.* 4:979–983.

Pokrywka, N., and E. C. Stephenson. 1991. Microtubules mediate the localization of *bicoid* RNA during *Drosophila* oogenesis. *Development.* 113:55–66.

Pollard, T. D., and R. D. Goldman. 1993. Cytoplasm and cell motility. *Curr. Opin. Cell Biol.* 5:1–2.

Ponte, P., P. Gunning, H. Blau, and L. Kedes. 1983. Human actin genes are single copy for alpha-skeletal and alpha-cardiac actin, but multicopy for beta- and gamma-cytoskeletal genes: 3′-untranslated regions are isotype specific, but are conserved in evolution. *Mol Cell. Biol.* 3:1783–1791.

Rastinejad, F., and H. Blau. 1993. Genetic complementation reveals a novel regulatory role for 3′-intranslated regions in growth and differentiation. *Cell.* 72:903–917.

Rastinejad, F., M. J. Conboy, T. A. Rando, and H. M. Blau. 1993. Tumor suppression by RNA from the 3′ untranslated region of α-tropomyosin. *Cell.* 75:1107–1117.

Sarndahl, E., M. Lindroth, T. Bengtsson, M. Fallman, J. Gustavsson, O. Stendahl, and T. Andersson. 1989. Association of ligand-receptor complexes with actin filaments in human neutrophils: a possible regulatory role for a G-protein. *J. Cell Biol.* 109:2791–2799.

Singer, R. H. 1992. The cytoskeleton and mRNA localization. *Curr. Opin. Cell Biol.* 4:15–19.

Singer, R. H. 1993. RNA zipcodes for cytoplasmic addresses. *Curr. Biol.* 3:719–721.

Sundell, C. L., and R. H. Singer. 1990. Actin mRNA localizes in the absence of protein synthesis. *J. Cell Biol.* 111:2397–2403.

Sundell, C. L., and R. H. Singer. 1991. Requirement of microfilaments in sorting actin messenger RNA. *Science (Wash. DC).* 253:1275–1277.

Theurkauf, W. E., S. Smiley, M. L. Wong, and B. M. Alberts. 1992. Reorganization of the cytoskeleton during *Drosophila* oogenesis: implications for axis specification and intracellular transport. *Development.* 115:923–936.

Wang, Y. 1987. Mobility of filamentous actin in the living cytoplasm. *J. Cell Biol.* 105:2811–2816.

Wharton, R. P., and G. Struhl. 1991. RNA regulatory elements mediate control of *Drosophila* body pattern by the posterior morphogen nanos. *Cell.* 67:955–967.

Yaffe, D., U. Nudel, Y. Mayer, and S. Neuman. 1985. Highly conserved sequences in the 3′ untranslated region of mRNAs coding for homologous proteins in distantly related species. *Nucleic Acids Res.* 13:3723–3737.

Yang, F., M. Demma, V. Warren, S. Dharmawardhane, and J. Condeelis. 1990. Identification of an actin-binding protein from *Dictyostelium* as elongation factor 1a. *Nature (Lond.)*. 347:494–496.

Yisraeli, J. K., S. Sokol, and D. A. Melton. 1990. A two-step model for the localization of maternal mRNA in *Xenopus* oocytes: involvement of microtubules and microfilaments in the translocation and anchoring of Vg-1 mRNA. *Development.* 108:289–298.